

Tuning of Thermo-Triggered Gel-to-Sol Transition of Aqueous Solution of Multi-Responsive Diblock Copolymer Poly(methoxytri(ethylene glycol) acrylate-co-acrylic acid)-*b*-poly(ethoxydi(ethylene glycol) acrylate)

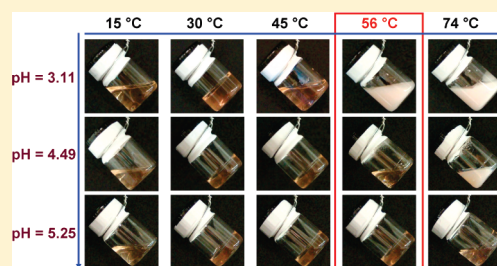
Naixiong Jin,[†] Jeremiah W. Woodcock,[†] Chenming Xue,[‡] Thomas G. O'Lenick,[†] Xueguang Jiang,[†] Shi Jin,[‡] Mark D. Dadmun,[†] and Bin Zhao^{†,*}

[†]Department of Chemistry, University of Tennessee, Knoxville, Tennessee 37996, United States

[‡]Department of Chemistry, College of Staten Island, CUNY, Staten Island, New York 10314, United States

S Supporting Information

ABSTRACT: This article reports on the synthesis of a hydrophilic diblock copolymer composed of two distinct thermosensitive polymers with one block containing a small amount of carboxylic acid groups, poly(methoxytri(ethylene glycol) acrylate-co-acrylic acid)-*b*-poly(ethoxydi(ethylene glycol) acrylate) (P(TEGMA-co-AA)-*b*-PDEGEA), and the study of thermo-induced sol–gel–sol transitions of its moderately concentrated aqueous solutions at various pH values. The diblock copolymer was obtained by the removal of *tert*-butyl groups of P(TEGMA-co-*tert*-butyl acrylate)-*b*-PDEGEA, which was synthesized by reversible addition–fragmentation chain transfer polymerization. PTEGMA and PDEGEA are thermosensitive polymers with lower critical solution temperatures (LCSTs) of 58 and 9 °C, respectively, in water. The incorporation of a small amount of carboxylic acid groups into PTEGMA allowed the LCST of the P(TEGMA-co-AA) block to be tuned by changing the solution pH. We found that a 20 wt % aqueous solution of P(TEGMA-co-AA)-*b*-PDEGEA with pH of 3.11 (measured at 0 °C) underwent multiple phase transitions upon heating, from a clear, free-flowing liquid (<19 °C) to a clear, free-standing gel (19 to 39 °C), to a clear, free-flowing hot liquid (40 to 55 °C), and to a cloudy mixture (≥56 °C). With the increase of pH, the gel-to-sol transition ($T_{\text{gel-sol}}$) and the clouding temperature (T_{clouding}) of the sample shifted to higher values, while the sol-to-gel transition temperature ($T_{\text{sol-gel}}$) remained the same. These transitions and the tunability of $T_{\text{gel-sol}}$ stemmed from the thermosensitive properties of the two blocks of the diblock copolymer and the pH dependence of the LCST of P(TEGMA-co-AA), which was confirmed by differential scanning calorimetry and dynamic light scattering studies. Using the vial inversion test method, we further mapped out the C-shaped sol–gel phase diagrams of (PTEGMA-co-AA)-*b*-PDEGEA in water in the moderate concentration range at three different pH values (3.11, 4.49, and 5.25, all measured at 0 °C). While the lower temperature boundaries overlapped, the upper temperature boundary shifted upward and the critical gelation concentration decreased with the increase of pH. In contrast, the sol–gel phase diagram of PTEGMA-*b*-PDEGEA, which contained no pH-responsive groups, showed no changes in $T_{\text{sol-gel}}$, $T_{\text{gel-sol}}$, and T_{clouding} with pH.



INTRODUCTION

Owing to the intriguing transitions between free-flowing liquids and free-standing gels and the associated changes in rheological properties, stimuli-induced reversible formation of aqueous micellar gels of block copolymers has received considerable interest.^{1–3} Compared with chemically cross-linked hydrogels, these responsive micellar gels, especially those triggered by temperature changes, can be more advantageous for certain applications because of the in situ sol–gel transition.^{1–3} For example, Jeong et al. reported injectable drug delivery systems based on aqueous solutions of block copolymers of poly(ethylene glycol) (PEO) and polylactide that can undergo cooling-induced sol–gel transitions.³ The polymer solutions were loaded with a model drug in the sol state at an elevated temperature. Upon subcutaneous injection and cooling to the

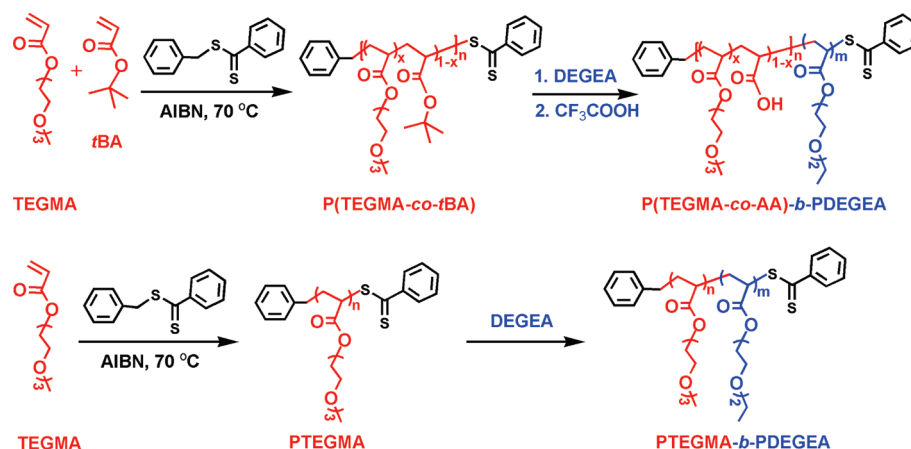
body temperature, the polymer solutions formed gels instantaneously that subsequently acted as matrices for sustained release of drug molecules.

Generally, there are two types of stimuli-responsive aqueous block copolymer micellar gels: 3-dimensional network gels, in which one block, e.g., the central block of an ABA triblock copolymer, forms bridges among micellar cores of other blocks,^{1a,4} and physically jammed micellar gels, in which discrete spherical micelles of block copolymers are packed into an ordered structure.^{1–3,5,6} Representative examples of the latter include aqueous gels of PEO-*b*-poly(propylene oxide)-*b*-PEO (PEO-*b*-PPO-*b*-PEO) triblock

Received: February 18, 2011

Revised: March 24, 2011

Published: April 04, 2011

Scheme 1. Synthesis of P(TEGMA-*co*-AA)-*b*-PDEGEA and PTEGMA-*b*-PDEGEA

copolymers.^{1,5} PPO is a thermosensitive water-soluble polymer exhibiting a lower critical solution temperature (LCST) in water at ~ 15 °C.^{1,7} Above the LCST, PEO-*b*-PPO-*b*-PEO self-assembles into micelles with the dehydrated PPO blocks associated into the core and PEO blocks forming the corona. At a sufficiently high concentration, i.e., above the critical gelation concentration (CGC), the aqueous solution of PEO-*b*-PPO-*b*-PEO undergoes sol–gel–sol transitions upon heating. The sol–gel phase diagram at low/moderate concentrations is usually a C-shaped curve.¹ It has been established that the sol-to-gel transition, corresponding to the lower temperature boundary in the phase diagram, is driven by the enhancement of micellization and the ordering of micelles with the increase of temperature, while the gel-to-sol transition, corresponding to the upper boundary, results from the shrinking of PEO at elevated temperatures. The ordered structures of micelles in the gel state have been confirmed by small-angle X-ray and neutron scattering studies.¹

Besides PEO-*b*-PPO-*b*-PEO triblock copolymers, other block copolymers that can form thermosensitive micellar gels in water have also been reported.^{2–4,6,8,9} For example, Aoshima et al. synthesized a series of well-defined vinyl ether block copolymers composed of two or more thermosensitive blocks with different LCSTs by living cationic polymerization.⁹ They observed that 20 wt % aqueous solutions of these block copolymers underwent multistage transitions from clear liquids to transparent gels, to hot clear liquids, and phase separated opaque mixtures upon heating. The sol-to-gel and gel-to-sol transitions are closely related to the LCSTs of the thermosensitive blocks.

We are especially interested in the active control of unimer-micelle and sol–gel transitions of thermosensitive hydrophilic block copolymers in water. Our strategy is to incorporate a small amount of stimuli-responsive groups into thermosensitive blocks of block copolymers such that the LCSTs of the thermosensitive blocks can be modified by applying an external stimulus.¹⁰ These doubly responsive block copolymers can undergo multiple micellization and dissociation transitions in dilute aqueous solutions and multiple sol–gel–sol transitions in moderately concentrated solutions in response to environmental variations. For example, we synthesized thermo- and light-responsive PEO-*b*-poly(ethoxytri(ethylene glycol) acrylate-*co*-*o*-nitrobenzyl acrylate) (PEO-*b*-P(TEGEA-*co*-NBA)) by atom transfer radical polymerization.^{10a} PTEGEA is a thermosensitive polymer with an LCST of 36 °C in water and *o*-nitrobenzyl group is known to

undergo a photocleavage reaction when exposed to 365 nm UV light.¹¹ The block copolymer dissolved molecularly in a 0.2 wt % aqueous solution when the temperature was below 25 °C and self-assembled into micelles at elevated temperatures. Upon UV irradiation, the *o*-nitrobenzyl groups were cleaved and the LCST of the thermosensitive block was increased, causing the micelles to dissociate. Further raising the temperature induced the formation of micelles again.^{10a} At a polymer concentration of 20 wt %, multiple sol–gel–sol transitions were achieved.^{10c} Such doubly responsive block copolymers are expected to offer more advantages for some potential applications compared with those that respond to only one external stimulus.

In this article, we report the synthesis of a well-defined hydrophilic diblock copolymer composed of two distinct thermosensitive polymers with the higher LCST block containing a small amount of carboxylic acid groups, poly(methoxytri(ethylene glycol) acrylate-*co*-acrylic acid)-*b*-poly(ethoxydi(ethylene glycol) acrylate) (P(TEGMA-*co*-AA)-*b*-PDEGEA), and the study of thermo-induced sol–gel–sol transitions of its moderately concentrated aqueous solutions at various pH values. PTEGMA and PDEGEA are thermosensitive water-soluble polymers with LCSTs of 58 and 9 °C, respectively, which belong to a new class of thermosensitive polymers with a short oligo-(ethylene glycol) pendant from each repeat unit.^{9,12} The block copolymer was prepared by reversible addition–fragmentation chain transfer polymerization (RAFT)¹³ and postpolymerization modification (Scheme 1). The incorporation of a small amount of carboxylic acid groups into PTEGMA allowed the LCST of the P(TEGMA-*co*-AA) block to be tuned by changing the solution pH. We show that the moderately concentrated aqueous solutions of this multiresponsive diblock copolymer undergo sol–gel–sol transitions upon heating and the gel-to-sol transition can be continuously tuned by adjusting the solution pH. It should be noted here that thermo- and pH-sensitive block copolymer aqueous gels have been reported in the literature.^{14–17} The block copolymers used in those studies were usually prepared by either growing pH-sensitive blocks from or introducing pH-responsive groups onto the chain ends of an ABA triblock copolymer that can form thermo-reversible gels in water (e.g., PEO-*b*-PPO-*b*-PEO).^{14–16} Other types of multiblock copolymers were also employed.¹⁷ We emphasize here that our thermo- and pH-sensitive polymer is a diblock copolymer and our block copolymer design, via the incorporation of a small amount of pH-responsive functional groups randomly

distributed in one block, is different, which allows the LCST to be readily tuned.

EXPERIMENTAL SECTION

Materials. Anisole (99%, anhydrous) and trifluoroacetic acid (99%) were purchased from Acros and used as received. Hexanes, diethyl ether, 1.0 M KOH solution (volumetric standard solution), and 1.0 M HCl solution (volumetric standard solution) were obtained from Fisher Scientific. Di(ethylene glycol) ethyl ether acrylate (or ethoxydi(ethylene glycol) acrylate, DEGEA, $\geq 90\%$, Aldrich) and *tert*-butyl acrylate (*t*BA, 99%, Fisher Scientific) were dried over calcium hydride overnight, distilled under reduced pressure, and stored in a refrigerator prior to use. Methoxytri(ethylene glycol) acrylate (TEGMA) was synthesized according to the procedure described in a previous publication.^{12f} 2,2'-Azobis(2-methylpropionitrile) (AIBN, 98%, Aldrich) was recrystallized in ethanol twice and dried under high vacuum at room temperature. The purified AIBN was then dissolved in *N,N*-dimethylformamide (DMF, extra dry, Acros) to make a solution with a concentration of 3.95 wt %. Benzyl dithiobenzoate, a chain transfer agent (CTA) used in RAFT, was synthesized according to a literature procedure¹⁸ and the molecular structure was confirmed by ¹H and ¹³C NMR spectroscopy. Twenty mM aqueous potassium hydrogen phthalate (KHP) buffers were made by dissolving KHP in Milli-Q water and the pH values were adjusted by adding either a 1.0 M aqueous KOH or a 1.0 M aqueous HCl solution. All pH values in this work were measured with a pH meter (Accumet AB15 pH meter from Fisher Scientific, calibrated with pH = 4.01, 7.00, and 10.01 standard buffer solutions) in an ice/water bath (0 °C). All other solvents and chemicals were purchased from either Aldrich or Fisher and used without further treatment.

Characterization. Size exclusion chromatography (SEC) was carried out at room temperature using PL-GPC 20 (an integrated GPC system from Polymer Laboratories, Inc.) with a refractive index detector, one PLgel 5 μ m guard column (50 \times 7.5 mm), and two PLgel 5 μ m mixed-C columns (each 300 \times 7.5 mm, linear range of molecular weight from 200 to 2 000 000 Da according to Polymer Laboratories, Inc.). The data were processed using Cirrus GPC/SEC software (Polymer Laboratories). Tetrahydrofuran was used as a carrier solvent at a flow rate of 1.0 mL/min. Polystyrene standards (Polymer Laboratories, Inc.) were employed for calibration. The ¹H NMR (300 MHz) spectra were recorded on a Varian Mercury 300 NMR spectrometer.

Synthesis of Macro-CTAs by RAFT. Below is a procedure for the synthesis of macro-CTA P(TEGMA-*co-t*BA) by RAFT. A similar procedure was used to prepare macro-CTA PTEGMA.¹⁹ Benzyl dithiobenzoate (21.4 mg, 0.088 mmol), 2,2'-azobis(2-methylpropionitrile) (AIBN, 34.6 mg of a solution of AIBN in DMF with a concentration of 3.95 wt %, 0.0083 mmol), *tert*-butyl acrylate (*t*BA, 0.297 g, 2.32 mmol), TEGMA (9.469 g, 43.4 mmol), and anisole (10.25 g) were added into a 50 mL two-necked flask. The mixture was stirred under a nitrogen atmosphere and degassed by three freeze–pump–thaw cycles. A sample was taken for ¹H NMR spectroscopy analysis, and the flask was placed in a 70 °C oil bath. The reaction was monitored by ¹H NMR spectroscopy and SEC analysis. After the polymerization proceeded for 255 min, the flask was removed from the oil bath and a sample was taken immediately for the determination of the monomer conversion by ¹H NMR spectroscopy. The reaction mixture was diluted with THF and precipitated in hexanes. The polymer was then dissolved in THF (10 mL) and precipitated in a mixture of hexane and diethyl ether (v:v = 60:40, 200 mL). This process was repeated an additional two times. The polymer was then dried in vacuum. SEC analysis results (polystyrene standards): $M_{n,SEC}$ = 28100 Da; polydispersity index (PDI) = 1.17. The DP of the copolymer was calculated from the monomer conversion and the monomer-to-CTA ratio. The peaks located in the range of 4.0–4.5 ppm, which were from $-CH_2OOC-$ of monomer TEGMA and the

TEGMA units in the copolymer, were used as internal standard. The conversion was calculated from the integral values of the peaks from 5.7 to 5.9 ppm ($CHH=CH-$ from both TEGMA and *t*BA monomers) at t = 0 and 255 min. The calculated DP was 194.

Synthesis of Diblock Copolymers by RAFT. Below is a procedure for the synthesis of P(TEGMA-*co-t*BA)-*b*-PDEGEA from macro-CTA P(TEGMA-*co-t*BA) by RAFT. A similar procedure was used to prepare PTEGMA-*b*-PDEGEA from macro-CTA PTEGMA.¹⁹ P(TEGMA-*co-t*BA) (2.834 g, 0.0686 mmol), AIBN (34.8 mg of a solution of AIBN in DMF with a concentration of 3.95 wt %, 0.0084 mmol), DEGEA (9.083 g, 48.3 mmol), and anisole (21.84 g) were added into a 50 mL two-necked flask. The mixture was stirred under a nitrogen atmosphere and then degassed by three freeze–pump–thaw cycles. A sample was taken for ¹H NMR spectroscopy analysis, and the flask was placed in a 70 °C oil bath. SEC and ¹H NMR spectroscopy were used to monitor the reaction progress. After the polymerization proceeded for 190 min, the polymerization was stopped by removing the flask from the oil bath and diluting the mixture with THF. The polymer solution was precipitated in hexanes. The polymer was then dissolved in THF (15 mL) and precipitated in a mixture of hexane and diethyl ether (v:v = 60:40, 200 mL). This process was repeated an additional two times. The block copolymer was then dried in vacuum and analyzed by ¹H NMR spectroscopy and SEC. SEC results (polystyrene standards): $M_{n,SEC}$ = 42300 Da; PDI = 1.20. The composition of the block copolymer was determined from the ¹H NMR spectrum. The obtained numbers of DEGEA, TEGMA, and *t*BA units were 95, 183 and 11, respectively.

Removal of *tert*-Butyl Groups of P(TEGMA-*co-t*BA)-*b*-PDEGEA. P(TEGMA-*co-t*BA)-*b*-PDEGEA (2.505 g, $M_{n,SEC}$ = 42300 Da, PDI = 1.20) was dissolved in dry dichloromethane (10 mL) in a 20 mL vial. After the addition of trifluoroacetic acid (2.34 g), the reaction mixture was stirred at room temperature for 48 h. The volatiles were then removed by the use of a rotavapor. The residue was dissolved in 100 mL of dichloromethane and the volatiles were evaporated again by a rotavapor. This process was repeated an additional two times to remove as much trifluoroacetic acid as possible. The polymer was then dissolved in THF (10 mL) and precipitated in a mixture of hexane and diethyl ether (v:v = 50:50, 100 mL) three times. After drying in vacuum, the polymer was obtained as a pink viscous liquid (2.30 g, yield: 92%). The successful removal of *tert*-butyl group was evidenced by the disappearance of the *tert*-butyl peak located at 1.4 ppm in the ¹H NMR spectrum.

Preparation of 20 wt % Aqueous Solution of P(TEGMA-*co-AA*)-*b*-PDEGEA. Below is a typical procedure for the preparation of a 20 wt % aqueous solution of P(TEGMA-*co-AA*)-*b*-PDEGEA. A similar procedure was used for the preparation of a 20 wt % aqueous solution of PTEGMA-*b*-PDEGEA.¹⁹ P(TEGMA-*co-AA*)-*b*-PDEGEA was added into a preweighed vial (inner diameter: 20 mm). The vial was then placed in a large flask and dried under high vacuum at 55 °C for 12 h. The mass of the dried polymer inside the vial was 0.584 g. Milli-Q water (2.334 g) was added into the vial. The mixture was then sonicated in an ice/water ultrasonic bath (Fisher Scientific Model B200 Ultrasonic Cleaner) to dissolve the polymer. The vial was then stored in a refrigerator (~ 4 °C) overnight and a homogeneous solution was obtained.

Rheological Measurements. Rheological experiments were conducted using a stress-controlled rheometer (TA Instruments Model TA AR 2000ex). A cone–plate geometry with a cone diameter of 20 mm and an angle of 2° (truncation 52 μ m) was employed; the temperature was controlled by the bottom Peltier plate. In each measurement, 90 μ L of a polymer solution was loaded onto the plate by a micropipet. The solvent trap was filled with water and a solvent trap cover was used to minimize water evaporation. Dynamic viscoelastic properties (dynamic storage modulus G' and loss modulus G'') of a polymer solution were measured by oscillatory shear experiments performed at a fixed frequency of 1 Hz in a heating ramp at a heating rate of 1 °C/min.

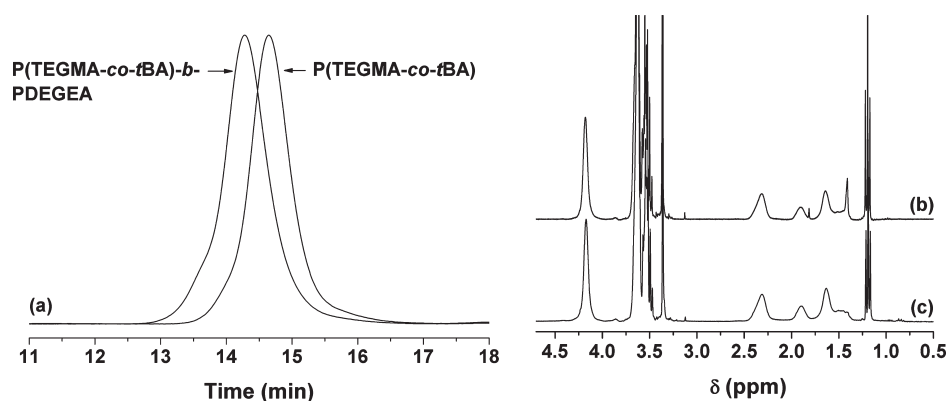


Figure 1. (a) Size exclusion chromatography traces of macro-CTA P(TEGMA-co-*t*BA) and diblock copolymer P(TEGMA-co-*t*BA)-*b*-PDEGEA, and ¹H NMR spectra of P(TEGMA-co-*t*BA)-*b*-PDEGEA (b) and P(TEGMA-co-AA)-*b*-PDEGEA (c). P(TEGMA-co-AA)-*b*-PDEGEA was prepared from P(TEGMA-co-*t*BA)-*b*-PDEGEA using trifluoroacetic acid to remove the *tert*-butyl groups. CDCl₃ was used as solvent in ¹H NMR spectroscopy analysis.

The frequency dependences of G' and G'' of a polymer solution at selected temperatures were obtained by frequency sweep tests from 0.1 to 100 Hz. A strain amplitude of $\gamma = 0.2\%$ was used in all dynamic tests to ensure that the deformation was within the linear viscoelastic regime. The flow properties (shear stress-shear rate curves) of a polymer solution at selected temperatures were measured by a shear rate ramp from 0 to 600 s⁻¹ for duration of 6 min. The apparent viscosities of a polymer solution at different temperatures were measured by a temperature ramp experiment performed at a heating rate of 3 °C/min and a shear rate of 10 s⁻¹.

Polarized Light Microscopy Experiments. Polarized light microscopy experiments were conducted on a Leica (DM LB2) polarized light microscope coupled with a Mettler hot stage (FP-90). The 20 wt % aqueous solution of P(TEGMA-co-AA)-*b*-PDEGEA was added into a thin (0.5 mm) quartz demountable cell. The temperature of the cell was controlled by a Mettler hot stage (FP-90).

Small-Angle X-ray Scattering Experiments. Small-angle X-ray scattering data were collected on a Bruker NanoStar equipped with a rotating anode X-ray generator and a Vantec 2000 area detector. Copper K_α radiation ($\lambda = 1.5418$ Å) was used. The 20 wt % aqueous solution of P(TEGMA-co-AA)-*b*-PDEGEA was loaded into a quartz capillary sample holder, which was then inserted into a cooling/heating stage. The temperature of the cooling/heating stage was controlled by a Materials Research Instruments TCPUP temperature controller. The scattering data for the samples were corrected by subtracting the background which was recorded from the same sample holder using deionized water. The calibration was performed using silver behenate as the standard sample.

Differential Scanning Calorimetry Study of Thermo-Induced Phase Transitions of Aqueous Solutions of P(TEGMA-co-AA)-*b*-PDEGEA. Differential scanning calorimetry analysis of polymer solutions was conducted on a TA Q-1000 DSC instrument that was calibrated with sapphire disks. Approximately 20 mg of a 20 wt % polymer solution was loaded into a preweighed aluminum hermetic pan and sealed carefully. A heating rate of 1 °C/min was used to obtain the thermograms with an empty pan as reference.

Dynamic Light Scattering Studies. Dynamic light scattering (DLS) studies of aqueous solutions of P(TEGMA-co-AA)-*b*-PDEGEA were conducted with a Brookhaven Instruments BI-200SM goniometer equipped with a PCI BI-9000AT digital correlator, a temperature controller, and a solid-state laser (model 25-LHP-928-249, $\lambda = 633$ nm) at a scattering angle of 90°. Three 0.02 wt % solutions of P(TEGMA-co-AA)-*b*-PDEGEA in 20 mM KHP aqueous buffers with pH values of 3.11, 4.49, and 5.25, respectively, were made. The solutions were filtered into borosilicate glass tubes with an inner diameter of 7.5 mm using Millipore hydrophilic PTFE filters (0.2 μm pore size) and the

tubes were sealed with PE stoppers. The glass tube was placed in the cell holder of the light scattering instrument and gradually heated. At each temperature, the solution was equilibrated for 20 min prior to data recording. The time intensity-intensity correlation functions were analyzed with a Laplace inversion program (CONTIN).

Determination of Sol–Gel–Sol–Cloudy Phase Diagrams of Diblock Copolymers in Water by the Vial Inversion Test and Visual Examination. A glass vial that contained an aqueous solution of a diblock copolymer with a known concentration was placed in the water bath of a Fisher Scientific Isotemp refrigerated circulator. The inner diameter of the vial was 20 mm. The temperature was gradually increased. At each temperature, the solution was equilibrated for 20 min before the vial was held in a tilted or inverted position for 5 s to visually examine if the solution was a mobile liquid or an immobile gel under its own weight. The temperature at which the solution changed from a mobile to an immobile state (or vice versa) was taken as the sol-to-gel (or gel-to-sol) transition temperature. The clouding temperature was determined by visual examination. Polymer solutions with different concentrations were obtained by adding a predetermined amount of water into the vial or evaporating water from the solution; their sol-to-gel/gel-to-sol transition temperatures and clouding temperatures were determined by the vial inversion method and visual examination.

RESULTS AND DISCUSSION

Synthesis of P(TEGMA-co-AA)-*b*-PDEGEA and P(TEGMA-co-tBA)-*b*-PDEGEA. P(TEGMA-co-AA)-*b*-PDEGEA, a diblock copolymer composed of two distinct thermosensitive polymers with the higher LCST PTEGMA block containing a small amount of carboxylic acid groups, was prepared by RAFT and subsequent removal of *tert*-butyl groups using trifluoroacetic acid (Scheme 1). The macro-CTA P(TEGMA-co-*t*BA) was synthesized by the copolymerization of TEGMA and *t*BA with a molar ratio of 100: 5.3 at 70 °C in anisole using benzyl dithiobenzoate as chain transfer agent and AIBN as initiator. P(TEGMA-co-*t*BA) was then used for the synthesis of the diblock copolymer. Figure 1a shows the SEC traces of P(TEGMA-co-*t*BA) and P(TEGMA-co-*t*BA)-*b*-PDEGEA. The peak completely shifted to the high molecular weight side and remained narrow. The polydispersity index (PDI) of the diblock copolymer using polystyrene calibration was 1.20. Figure 1b shows the ¹H NMR spectrum of P(TEGMA-co-*t*BA)-*b*-PDEGEA. The numbers of TEGMA, *t*BA, and DEGEA units in the block copolymer were calculated using the integral values of the peak from 4.4 to

Table 1. Characterization Data for P(TEGMA-*co*-*t*BA), P(TEGMA-*co*-*t*BA)-*b*-PDEGEA, P(TEGMA-*co*-AA)-*b*-PDEGEA, PTEGMA, and PTEGMA-*b*-PDEGEA

polymer ^a	$M_{n,SEC}$ (Da), PDI ^b	n_{TEGMA}^c	
		n_{tBA} (or AA): n_{DEGEA}	
P(TEGMA- <i>co</i> - <i>t</i> BA)	28100, 1.17	183:11:0	
P(TEGMA- <i>co</i> - <i>t</i> BA)- <i>b</i> -PDEGEA	42300, 1.20	183:11:95	
P(TEGMA- <i>co</i> -AA)- <i>b</i> -PDEGEA	NA	183:11:95	
PTEGMA	24500, 1.15	166:0:0	
PTEGMA- <i>b</i> -PDEGEA	41100, 1.23	166:0:106	

^a P(TEGMA-*co*-*t*BA), PTEGMA, P(TEGMA-*co*-*t*BA)-*b*-PDEGEA, and PTEGMA-*b*-PDEGEA were synthesized by RAFT; P(TEGMA-*co*-AA)-*b*-PDEGEA was obtained from P(TEGMA-*co*-*t*BA)-*b*-PDEGEA by the removal of *tert*-butyl groups using trifluoroacetic acid. ^b The values of $M_{n,SEC}$ and PDI of polymers were determined by size exclusion chromatography using polystyrene calibration. ^c The degrees of polymerization of macro-CTAs P(TEGMA-*co*-*t*BA) and PTEGMA were calculated from the monomer conversion and monomer-to-CTA ratio. The numbers of TEGMA, *t*BA, and DEGEA units in the copolymers were determined from ¹H NMR spectra along with the use of the DPs of macro-CTAs.

4.0 ppm ($-\text{CH}_2\text{OOC}-$ of TEGMA and DEGEA units), the peak from 2.5 to 2.1 ppm ($-\text{CH}_2\text{CH}-$ of TEGMA, DEGEA and *t*BA units), and the peaks from 1.3 to 1.1 ppm ($-\text{CH}_2\text{CH}_3$ of DEGEA units) along with the DP of macro-CTA P(TEGMA-*co*-*t*BA) (DP = 194). The obtained numbers of TEGMA, *t*BA, and DEGEA units were 183, 11, and 95, respectively. The molar ratio of TEGMA and *t*BA units in the copolymer was 100: 6.0, close to the feed ratio of 100: 5.3 in the synthesis of macro-CTA P(TEGMA-*co*-*t*BA).

The *tert*-butyl groups of P(TEGMA-*co*-*t*BA)-*b*-PDEGEA were then removed by using trifluoroacetic acid, yielding the targeted thermo- and pH-sensitive diblock copolymer, P(TEGMA-*co*-AA)-*b*-PDEGEA. This was confirmed by ¹H NMR spectroscopy analysis; the *tert*-butyl peak located at 1.4 ppm disappeared after the reaction (Figure 1c). The block copolymer was then used for micellar gel study. For comparison, PTEGMA-*b*-PDEGEA, which did not contain pH-responsive groups, was also synthesized by RAFT (Scheme 1).¹⁹ The characterization data for the polymers used in this work are summarized in Table 1.

Thermo-Induced Sol–Gel–Sol–Cloudy Transitions of 20 wt % Aqueous Solution of P(TEGMA-*co*-AA)-*b*-PDEGEA with pH of 3.11. A 20 wt % aqueous solution of P(TEGMA-*co*-AA)-*b*-PDEGEA was made by dissolving the polymer in Milli-Q water and the pH of the solution at 0 °C was 3.11.²⁰ To test the thermo-induced sol–gel–sol transitions, we gradually heated the solution from 8 °C. At each temperature, the sample was equilibrated for 20 min before the vial was tilted or inverted to visually examine if the sample was a free-flowing liquid or an immobile micellar gel under its own weight. As shown in Figure 2, the sample was a free-flowing liquid at 15 °C. With the increase of temperature, the sample turned into a clear gel at 19 °C, which was 10 °C higher than the cloud point of PDEGEA (Figure 1b shows the sample at 30 °C). Further increasing the temperature to 40 °C, the solution began to flow under its own weight when tilted but remained clear, indicating a transition from the gel to a sol (Figure 1c shows the sample at 45 °C). The block copolymer solution remained clear until the temperature reached 56 °C, at which point it turned cloudy (Figure 1d). This clouding temperature was very close to the cloud point of PTEGMA in water at a concentration of 0.5 wt % (58 °C).^{12f} The sample stayed

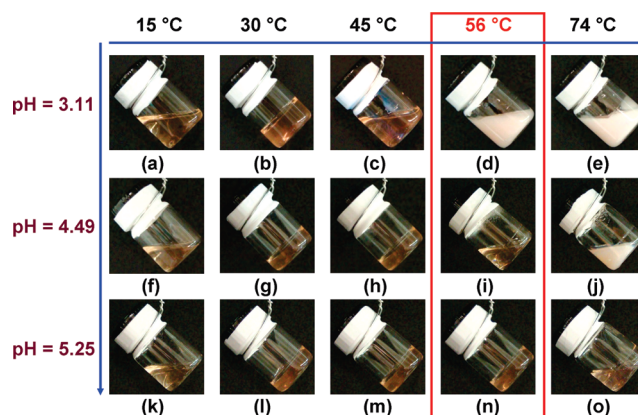


Figure 2. Digital optical pictures of 20 wt % aqueous solutions of P(TEGMA-*co*-AA)-*b*-PDEGEA at pH = 3.11 (the first row), 4.49 (the second row), and 5.25 (the third row), and $T = 15$ °C (the first column, a, f, k), 30 °C (the second column, b, g, l), 45 °C (the third column, c, h, m), 56 °C (the fourth column, d, i, n), and 74 °C (the fifth column, e, j, o).

cloudy after that (Figure 1e shows the picture of the sample at 74 °C). Evidently, the sol-to-gel and the clear-to-cloudy transition temperatures were close to the LCSTs of the two component blocks of P(TEGMA-*co*-AA)-*b*-PDEGEA.

Rheological Properties of 20 wt % Aqueous Solution of P(TEGMA-*co*-AA)-*b*-PDEGEA with pH of 3.11. Rheological measurements were conducted to characterize the thermo-induced sol–gel/gel–sol transitions of the 20 wt % aqueous solution of P(TEGMA-*co*-AA)-*b*-PDEGEA with pH of 3.11 and the gel property. Figure 3a shows the dynamic storage modulus G' and loss modulus G'' of the sample as a function of temperature collected from an oscillatory shear experiment, which was performed at a fixed frequency of 1 Hz in a heating ramp at a heating rate of 1 °C/min. A strain amplitude of $\gamma = 0.2\%$ was used to ensure that the measurements were taken in the linear viscoelastic regime. Below ~ 15 °C, both G' and G'' were very small. When the temperature was raised above 15 °C, G' and G'' increased quickly and G' became larger than G'' at ~ 21 °C, suggesting that the sample turned into a gel. In the temperature range of 23 to 37 °C, the G' was greater than G'' by at least 1 order of magnitude. Moreover, the G' was nearly independent of frequency. These are characteristics of gels. Above 37 °C, G' and G'' began to decrease and a sharp drop was observed for both moduli at ~ 39 °C. The crossover points of the two curves are commonly used as indicators of sol-to-gel ($T_{\text{sol-gel}}$) and gel-to-sol transitions ($T_{\text{gel-sol}}$).^{1,21} Thus, with this method, the $T_{\text{sol-gel}}$ and the $T_{\text{gel-sol}}$ were 21.1 and 40.8 °C, respectively, which were close to those determined by the vial inversion method (19 and 40 °C).

The difference in the rheological property of the sample below and above $T_{\text{sol-gel}}$ can also be seen from the results of frequency sweep experiments (Figure 4). At 16 °C, which was below the $T_{\text{sol-gel}}$, G' scaled with the second power of oscillation frequency f , while G'' increased linearly with f (Figure 4a). This is the typical rheological behavior of a viscoelastic fluid.^{9d,21} At 25 °C, G' was essentially independent of f and G'' varied slightly with a minimum appearing at an intermediate frequency (Figure 4b). In addition, G' was about 1 order of magnitude larger than G'' in the frequency range of 0.1 to ~ 50 s^{−1}. These are the characteristics of elastic solids with a cubic structure,^{1,22} which is also supported by the polarized light microscopy result. In the gel zone, the sample was completely dark under a polarized light

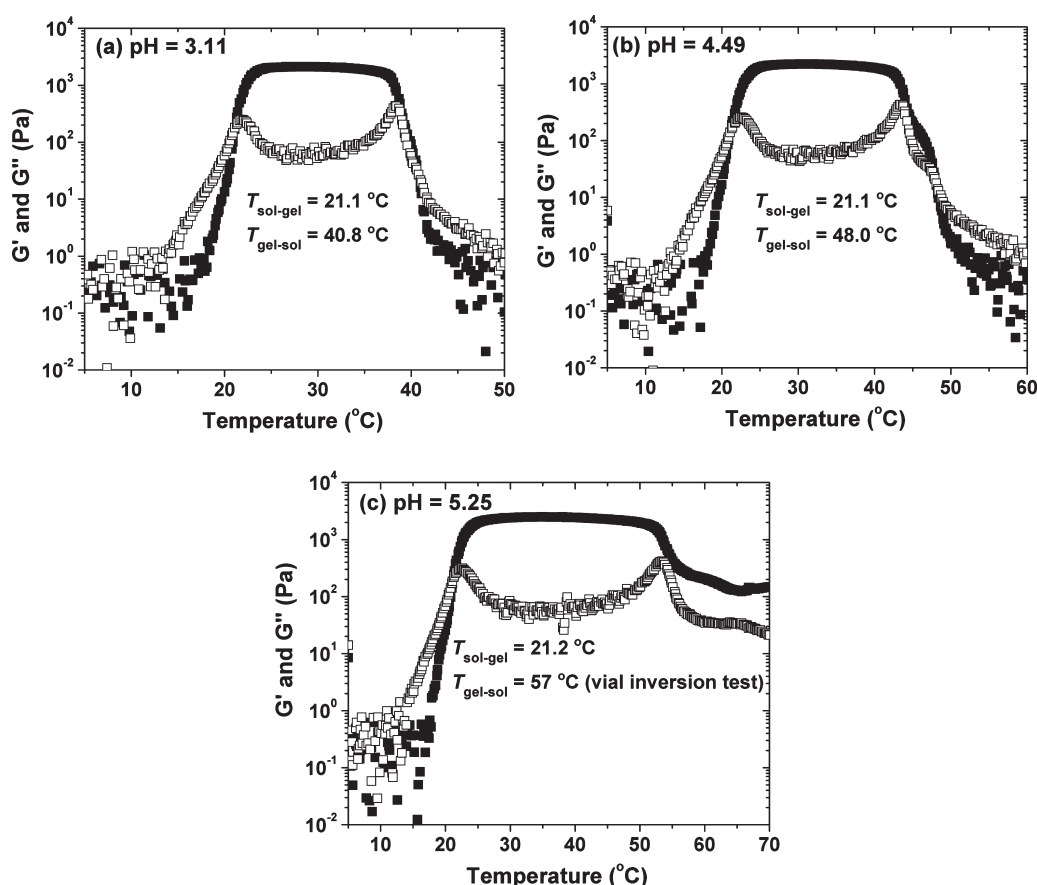


Figure 3. Plot of dynamic storage modulus G' (■) and loss modulus G'' (□) of 20 wt % aqueous solution of P(TEGMA-co-AA)-b-PDEGEA with pH of (a) 3.11, (b) 4.49, and (c) 5.25 versus temperature. The data were collected from oscillatory shear experiments performed in a heating ramp using a heating rate of 1 °C/min, a strain amplitude of 0.2%, and a frequency of 1 Hz.

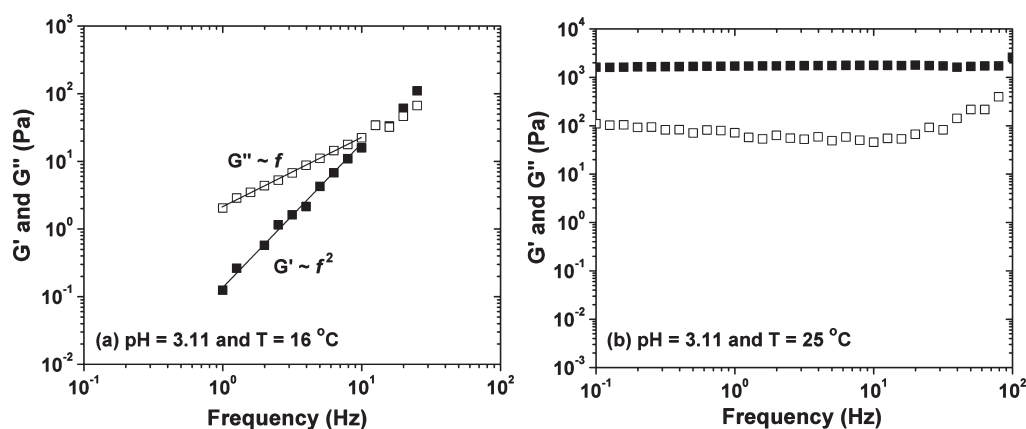


Figure 4. Frequency dependences of dynamic storage modulus G' (■) and dynamic loss modulus G'' (□) of the 20 wt % aqueous solution of P(TEGMA-co-AA)-b-PDEGEA with pH of 3.11 at (a) 16 and (b) 25 °C. A strain amplitude of 0.2% was used in the frequency sweep experiments.

microscope with crossed polarizers, demonstrating that the gel was optically isotropic.

Figure 5a shows the flow curves (plots of shear stress versus shear rate) of the sample with pH of 3.11 at various temperatures. At 10, 12, and 15 °C, the shear stress σ was proportional to the shear rate dy/dt , indicating that the sample behaved as a Newtonian liquid. From 25–39 °C, the sample exhibited plastic flow behavior;^{9d} after the initial resistance was overcome, the shear

stress increased linearly with the shear rate. At 50 °C, the sample again behaved as a Newtonian liquid. These observations were consistent with the results from visual examination and dynamic viscoelastic measurements. The temperature dependence of apparent viscosity of the sample collected at a shear rate of 10 s⁻¹ is displayed in Figure 5b. When the temperature was below 13 °C, the viscosity was ≤ 0.05 Pa·s and there was essentially no change from 5 to 13 °C. A sharp increase was observed at

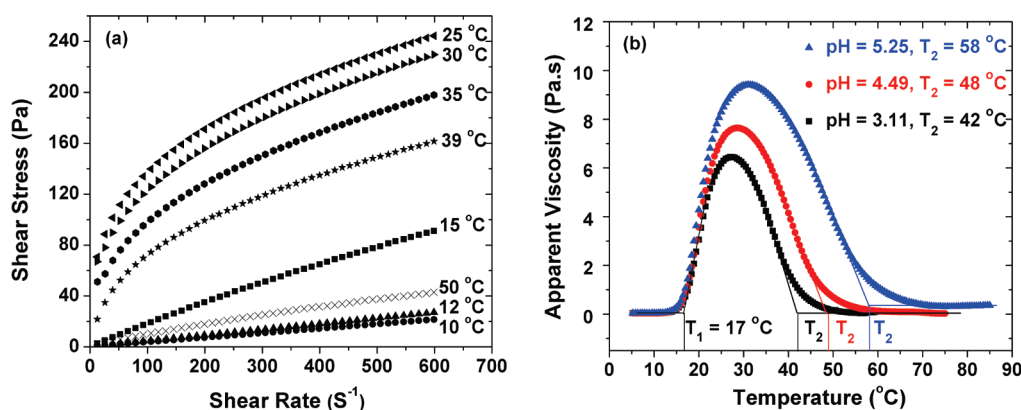


Figure 5. (a) Flow curves of the 20 wt % aqueous solution of P(TEGMA-*co*-AA)-*b*-PDEGEA with pH of 3.11 at various temperatures, and (b) apparent viscosity of the sample as a function of temperature at pH of 3.11 (■), 4.49 (●), and 5.25 (▲), collected at a shear rate of 10 s⁻¹ and a heating rate of 3 °C/min.

~20 °C, which was around the $T_{\text{sol-gel}}$ (19 °C by visual examination and 21.1 °C from rheological measurement). After reaching the highest value, 6.45 Pa·s, at 27 °C, the apparent viscosity began to decrease with the further increase of temperature. At 55 °C, the apparent viscosity was only 0.051 Pa·s. The transition temperatures determined from Figure 5b, $T_1 = 17$ °C and $T_2 = 42$ °C, matched reasonably well with those from the vial inversion test and the rheological measurement.

pH Effect on Sol–Gel–Sol-Cloudy Transitions of 20 wt % Aqueous Solution of P(TEGMA-*co*-AA)-*b*-PDEGEA. The LCST of a thermosensitive water-soluble polymer that contains a small amount of weak acid groups is known to depend on the solution pH.²³ With the increase of pH, the weak acid groups ionize, making the polymer more hydrophilic and thus increasing the LCST. For the diblock copolymer studied here, the higher LCST block contained 5.7 mol % of AA. To study the pH effects on sol–gel–sol transitions, clouding temperature, and gel property, we raised the pH of the 20 wt % aqueous solution of P(TEGMA-*co*-AA)-*b*-PDEGEA in a stepwise fashion by injecting a 1.0 M KOH solution. Each time, the sample was sonicated in an ice/water bath for 2 min to ensure that the solution was homogeneous and the pH was measured at 0 °C.

Figure 6 shows the $T_{\text{sol-gel}}$, $T_{\text{gel-sol}}$ and T_{clouding} of the sample, determined by visual examination, as a function of pH.²⁰ The $T_{\text{sol-gel}}$ remained at 19 °C throughout the studied pH range (3.11–6.04), consistent with the expected as the $T_{\text{sol-gel}}$ of the sample was governed by the thermosensitive property of the lower LCST block – the PDEGEA block that did not contain any pH-sensitive groups. In contrast, the $T_{\text{gel-sol}}$ and the T_{clouding} increased with the increase of pH. Initially, the $T_{\text{gel-sol}}$ changed slowly with pH, from 40 °C at pH = 3.11 to 47 °C at pH 4.49. Above pH = 4.49, the increase became faster; in 1.6 pH units, the $T_{\text{gel-sol}}$ jumped up by 30 °C ($T_{\text{gel-sol}} = 77$ °C at pH = 6.04). Interestingly, the T_{clouding} went up with pH more sharply than the $T_{\text{gel-sol}}$. The difference between $T_{\text{gel-sol}}$ and T_{clouding} became larger with the increase of pH, from 16 °C at pH = 3.11, to 25 °C at pH 4.23, and to 40 °C at pH = 4.81. At pH of 5.08, the clouding temperature was not observed in the studied temperature range (up to 97 °C). To confirm that the tunability of $T_{\text{gel-sol}}$ and T_{clouding} arose from the pH dependence of the LCST of P(TEGMA-*co*-AA), we measured the cloud points of P(TEGMA-*co*-AA), which was obtained from macro-CTA P-(TEGMA-*co*-tBA) by the removal of *tert*-butyl groups, in 10 mM aqueous KHP buffers with various pH values at a concentration of 0.5 wt %. The cloud point of P(TEGMA-*co*-AA) in the dilute

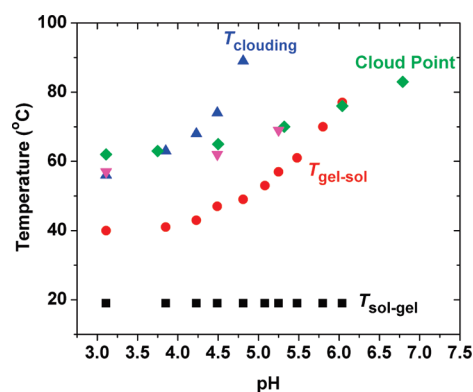


Figure 6. Sol-to-gel transition temperature ($T_{\text{sol-gel}}$ ■), gel-to-sol transition temperature ($T_{\text{gel-sol}}$ ●), and clouding temperature (T_{clouding} ▲) of the 20 wt % aqueous solution of P(TEGMA-*co*-AA)-*b*-PDEGEA as a function of pH as well as the pH dependences of the cloud point of random copolymer P(TEGMA-*co*-AA) at a concentration of 0.5 wt % in the 10 mM KHP aqueous buffer (◆) and the clouding temperature of P(TEGMA-*co*-AA)-*b*-PDEGEA at a concentration of 0.02 wt % in the 20 mM KHP aqueous buffer (▼).

aqueous solution increased smoothly from 62 °C at pH = 3.11 to 83 °C at pH = 6.79 (Figure 6). However, the increase was slower compared with the $T_{\text{gel-sol}}$ and the T_{clouding} . Figure 6 also shows that the $T_{\text{gel-sol}}$ is closely related to but not solely determined by the LCST of P(TEGMA-*co*-AA). The PEO type thermosensitive water-soluble polymers are known to undergo shrinking, though small, with the increase of temperature.^{1,24} The gel-to-sol transition occurred when the effective volume of micelles dropped below the critical value for the gelation.

The pH effect on gel-to-sol and clouding transitions of the 20 wt % aqueous solution of P(TEGMA-*co*-AA)-*b*-PDEGEA can be easily seen from the pictures of the sample in Figure 2. At 45 °C, the sample was a free-flowing clear sol when the pH was 3.11 (Figure 2c) but became a free-standing, clear gel at pH = 4.49 (Figure 2h). Interestingly, three distinct states, cloudy sol (Figure 2d), clear sol (Figure 2i), and clear gel (Figure 2n), were observed at 56 °C under the three different pH values.

The dynamic rheological properties of the samples at pH values of 4.49 and 5.25 were investigated and the data are shown in Figure 3. Consistent with the results from the visual examination, the values of $T_{\text{sol-gel}}$ at pH of 4.49 and 5.25 were the same as

that at pH = 3.11. With the increase of pH from 3.11 to 4.49, the gel zone clearly became wider and the $T_{\text{gel-sol}}$ shifted to a higher temperature (48.0 °C). For the pH of 5.25, although the G' and G'' curves did not cross over each other at elevated temperatures,²⁵ the plateau zone of G' was significantly broader than those at pH values of 3.11 and 4.49, indicating that the $T_{\text{gel-sol}}$ shifted to a higher temperature ($T_{\text{gel-sol}}$ = 57 °C by visual examination). Interestingly, we also found that the maximum value of G' increased with the increase of pH, from 2119 Pa at pH = 3.11, to 2231 Pa at pH = 4.49, and 2469 Pa at pH of 5.25. This is likely because the ionization of carboxylic acid groups at higher pH values causes the volume fraction of micelles to increase and thus the micelles are more jammed in the gel state, resulting in higher G' values.

The pH effect can also be seen from the flow curves of the sample at three different pH values. At 50 °C, the solution with the original pH of 3.11 was a Newtonian liquid (Figure 5a), while at pH = 5.25, it exhibited a plastic flow behavior at the same temperature.¹⁹ Similarly, at 55 °C, the sample was a free-flowing liquid at pH = 4.49 but became a gel with a finite yield stress at pH = 5.25.¹⁹ Besides the viscosity data for pH = 3.11, Figure 5b also shows the plots of apparent viscosity versus temperature for pH = 4.49 and 5.25. The three curves overlapped on the left side and the T_1 defined in the figure was essentially identical for three pH values, indicating that the pH change had no effect on the $T_{\text{sol-gel}}$ of the sample, consistent with the results in Figures 3 and 6. Noticeable differences were observed on the right sides of the curves; T_2 shifted to higher temperatures with the increase of pH, from 42 °C at pH = 3.11, to 48 °C for pH = 4.49, and 58 °C for pH = 5.25. These temperatures were close to the corresponding gel-to-sol transitions by visual examination (40, 47, and 57 °C, respectively). Moreover, the highest value of the apparent viscosity increased with the pH and also appeared at a higher temperature, from 6.45 Pa·s at 27 °C for pH = 3.11, to 7.64 Pa·s observed at 28.5 °C for pH = 4.49, and to 9.41 Pa·s that appeared at 31 °C for pH = 5.25. These observations suggested that the gel was slightly harder at a higher pH value, in agreement with the observation from dynamic viscoelastic measurements that the maximum value of G' increased slightly with the increase of the solution pH.

Differential Scanning Calorimetry and Dynamic Light Scattering Studies of pH Effects on Solution Behavior of P(TEGMA-co-AA)-b-PDEGEA. The observed solution behavior of the 20 wt % aqueous solution of P(TEGMA-co-AA)-b-PDEGEA stemmed from the thermosensitive properties of the two blocks and the pH dependence of the LCST of P(TEGMA-co-AA). Below the LCST of PDEGEA ($\text{LCST}_{\text{PDEGEA}}$), the block copolymer dissolved molecularly in water. Above the $\text{LCST}_{\text{PDEGEA}}$, the polymer molecules self-assembled into micelles with the dehydrated PDEGEA blocks associated into the core and the P(TEGMA-co-AA) blocks forming the corona. With the increase of temperature, more block copolymer molecules entered the micelles. When the effective volume of micelles exceeded a critical value, the solution turned into a gel. Like other PEO-type thermosensitive polymers,^{1,24} the copolymer underwent shrinking at elevated temperatures. At a certain point, the volume fraction of micelles dropped below the critical value, triggering the transition from a clear gel to a clear sol. At an even higher temperature, the P(TEGMA-co-AA) blocks underwent a LCST transition and macroscopically, the clear sol turned into a cloudy mixture. When the solution pH was raised, the carboxylic acid groups ionized, causing the P(TEGMA-co-AA) block to be more hydrophilic. As a result, the LCST transition occurred at a higher temperature and so did the gel-to-sol transition and the clouding transition.

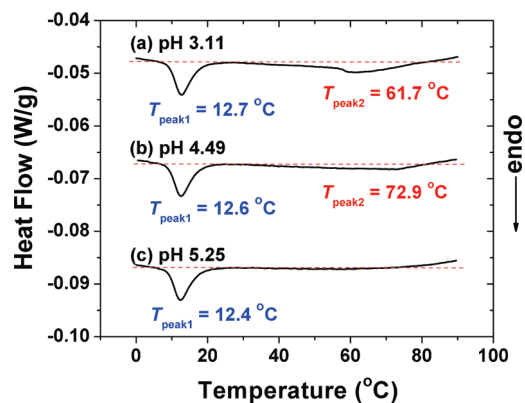


Figure 7. Differential scanning calorimetry thermograms of 20 wt % aqueous solutions of P(TEGMA-co-AA)-b-PDEGEA with pH of 3.11 (a), 4.49 (b), and 5.25 (c). The heating rate was 1 °C/min. For the sake of clarity, the thermograms were shifted vertically.

To look into the origin of the observed pH effects on sol–gel–sol–cloudy transitions, we conducted differential scanning calorimetry (DSC) analysis of the 20 wt % aqueous solution of P(TEGMA-co-AA)-b-PDEGEA and dynamic light scattering (DLS) studies of 0.02 wt % aqueous solutions of the block copolymer with three different pH values (3.11, 4.49, and 5.25). Figure 7a shows the DSC thermogram of the sample with pH of 3.11. Two endothermic peaks were observed with the peak positions located at 12.7 and 61.7 °C, indicating that the transitions were entropically driven, consistent with the commonly accepted mechanism for the LCST behavior of thermosensitive water-soluble polymers.^{9d,26} The two peaks, which were reasonably close to the $T_{\text{sol-gel}}$ (19 °C) and the T_{clouding} (56 °C) of the sample by visual examination, respectively, were attributed to the LCST transitions of the two thermosensitive blocks, PDEGEA and P(TEGMA-co-AA), of the block copolymer. While the peak at the lower temperature was relatively sharp, suggesting a strong phase transition, the one at the higher temperature was broad, a sign of a weaker phase transition. As discussed by Feil et al., the amount of structured water around a thermosensitive water-soluble polymer is a function of temperature and the LCST transition at a higher temperature tends to be broader and weaker.^{23b}

With the increase of pH from 3.11 to 4.49 and 5.25, the peak of the PDEGEA block remained essentially at the same position as expected. For the sample with pH of 4.49, the endothermic peak position of the P(TEGMA-co-AA) block shifted to 72.9 °C and the transition became even broader (Figure 7b). This observation is in line with that reported by Urry.²⁷ The ionization of carboxylic acid groups introduced charges onto the thermosensitive block and disrupted the ordered structure of water molecules around the hydrophobic moieties. In addition, the random distribution of a small amount of carboxylic acid groups further enhanced the heterogeneity, resulting in a broader transition. The maximum peak position, 72.9 °C, was close to the clouding temperature, 74 °C, from visual examination. At pH of 5.25, the endothermic peak at the higher temperature was not observed in the studied temperature range. These results were consistent with the observations from the visual examination and rheological measurements that the $T_{\text{sol-gel}}$ remained the same while the $T_{\text{gel-sol}}$ and T_{clouding} shifted to higher temperatures with the increase of pH, evidencing that the sol–gel–sol–cloudy transitions originated from the thermosensitive properties of the two

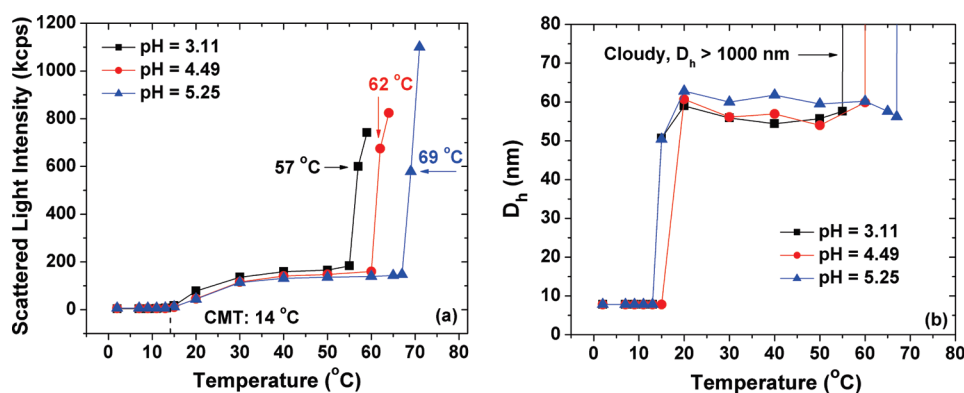


Figure 8. Scattering intensity at scattering angle of 90° (a) and apparent hydrodynamic size D_h (b), obtained from CONTIN analysis, as a function of temperature in a dynamic light scattering study of a 0.02 wt % solution of P(TEGMA-*co*-AA)-*b*-PDEGEA in a 20 mM aqueous KHP buffer with pH = 3.11 (■), 4.49 (●), and 5.25 (▲).

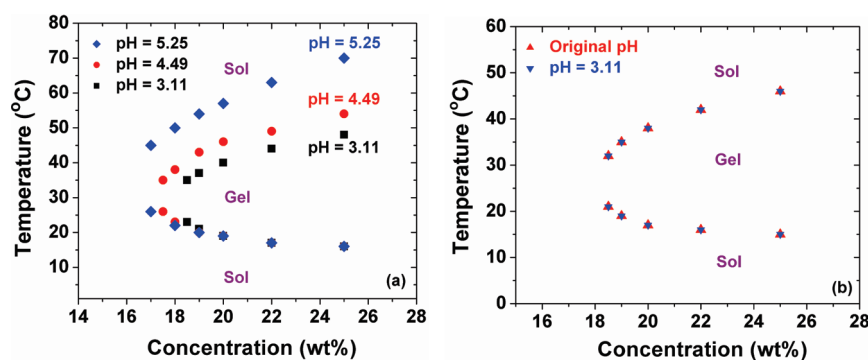


Figure 9. Sol–gel phase diagrams determined by the vial inversion test method for (a) P(TEGMA-*co*-AA)-*b*-PDEGEA in water at pH of 3.11 (■), 4.49 (●), and 5.25 (◆) and for (b) PTEGMA-*b*-PDEGEA in water at the original pH (▲) and pH of 3.11 (▼).

blocks and the pH dependence of the LCST transition of the P(TEGMA-*co*-AA) block.

Figure 8 shows the DLS results. For the 0.02 wt % solution of P(TEGMA-*co*-AA)-*b*-PDEGEA in a 20 mM KHP aqueous buffer with pH of 3.11, below 14 °C, the scattering intensity was low and the apparent size was <10 nm, indicating that the block copolymer dissolved molecularly in water. With the increase of temperature, the scattering intensity increased and micelles with an apparent hydrodynamic size of ~55 nm were observed in the temperature range of 15 to 55 °C. The critical micellization temperature (CMT) was 14 °C. When the temperature reached 57 °C, the scattering intensity jumped up dramatically and aggregates of >1000 nm were found from the DLS analysis; this temperature corresponded to the LCST transition of P(TEGMA-*co*-AA) and matched the T_{clouding} (56 °C) very well.

With the increase of pH from 3.11 to 4.49 and 5.25, the CMT did not change (Figure 8a). The second transition temperature at which large aggregates were observed shifted from 57 °C at pH = 3.11, to 62 °C at pH = 4.49, and 69 °C at pH = 5.25. Note that the increase of the clouding temperature of 0.02 wt % aqueous solutions of P(TEGMA-*co*-AA)-*b*-PDEGEA with pH was similar to that of 0.5 wt % aqueous solutions of P(TEGMA-*co*-AA), but quite different from the trend of 20 wt % aqueous solutions of P(TEGMA-*co*-AA)-*b*-PDEGEA (Figure 6). This observation suggests that the rather rapid increase in the clouding temperature with the increase of pH for the 20 wt % aqueous solution of P(TEGMA-*co*-AA)-*b*-PDEGEA was likely a result of the high

micelle concentration. From the DSC and DLS results presented above, it is clear that the sol–gel–sol–cloudy transitions originated from the responsive properties of the two blocks.

Sol–Gel–Sol Phase Diagrams of P(TEGMA-*co*-AA)-*b*-PDEGEA in Water at Moderate Concentrations. We further mapped out the sol–gel–sol phase diagrams for the moderately concentrated aqueous solutions of P(TEGMA-*co*-AA)-*b*-PDEGEA at three different pH values (pH = 3.11, 4.49, and 5.25).²⁰ The results are shown in Figure 9a and all three diagrams are C-shaped curves. It should be noted here that in the process of changing the polymer concentration by evaporating or adding water for the samples with pH of 3.11, we measured the pH value for each concentration and found that the pH was in the range of 3.07–3.11 when the polymer concentration was changed between 18 to 25 wt %. Thus, the effect of pH variations from the change of the polymer concentration on the sol–gel/gel–sol transitions should be quite small. One noticeable feature in Figure 9a is that the lower temperature boundaries for the three pH values overlapped while the upper temperature boundary shifted upward with the increase of pH. The gap between any two curves appeared to be either essentially independent of concentration or increase slightly with the increase of polymer concentration. Different from $T_{\text{sol–gel}}$ and $T_{\text{gel–sol}}$, the clouding temperature at a specific pH value did not change with the polymer concentration in the studied concentration range (T_{clouding} remained at 56 °C for pH of 3.11 and 74 °C for pH of 4.49). The fact that there was a difference between clouding

temperature and $T_{\text{gel-sol}}$ indicates that the gel-to-sol transition was not entirely and directly governed by the LCST transition. The gel-to-sol transition occurred when the volume fraction of micelles dropped below the critical value. Although the continued dehydration of PDEGEA blocks in the micellar cores at elevated temperatures could contribute, we believe that the change in the micelle volume fraction mainly came from the shrinking of the corona blocks. Figure 9b shows the C-shaped sol-gel-sol phase diagram of P(TEGMA-*b*-PDEGEA in the moderate concentration range at the original neutral pH value. To compare its solution behavior with that of P(TEGMA-*co*-AA)-*b*-PDEGEA, we injected a 1.0 M HCl aqueous solution to adjust the pH to 3.11 and determined the sol-gel-sol phase diagram. The two diagrams overlapped, indicating that the change of pH to 3.11 had no effect on the sol-gel-sol transitions as expected.

A second noticeable feature of Figure 9a is that the curve not only shifted upward but also extended into the lower concentration range with the increase of pH. That is, the critical gelation concentration (CGC) decreased with the increase of pH, from ~18 wt % at pH 3.11, to ~17 wt % at pH = 4.49, to ~16 wt % at pH = 5.25. This is reasonable because at a higher pH the carboxylic acid groups ionize, producing charges on the P(TEGMA-*co*-AA) block. Two scenarios can be envisioned.²⁸ (i) The micelle size increases slightly with the increase of pH because of the charge-charge interaction in the corona layer while the number of polymer molecules in each micelle stays about the same. (ii) The number of polymer molecules in each micelle decreases with the increase of pH while the apparent hydrodynamic size stays about the same or decreases slightly. Thus, more micelles would be present in the solution. Either of these two scenarios would lead to a greater volume fraction of micelles at a higher pH value.

Although the DLS studies of 0.02 wt % aqueous solutions of P(TEGMA-*co*-AA)-*b*-PDEGEA showed that the apparent diameter of micelles appeared to be larger at higher pH values (Figure 8), the situation for the 20 wt % block copolymer solution might be different. We conducted small-angle X-ray scattering studies of the samples with pH values of 3.11, 4.49, and 5.25 at 25 °C. The results and analysis are included in the Supporting Information. Clear diffraction spots were observed in the 2-dimensional scattering patterns of the samples with pH of 4.49 and 5.25, demonstrating that the micelles were packed into an ordered state and the crystalline domains were fairly large. Considering the similarity between the one-dimensional scattering curves integrated from the 2-D patterns for pH of 3.11 and 5.25, the micelles in the pH 3.11 sample were also likely in the ordered state but the crystalline domains were much smaller. We found that the diffraction spots could be explained by using a combination of face-centered cubic (FCC) and body-centered cubic (BCC) lattices (i.e., some micelles crystallized into an FCC structure while others into an BCC lattice). After indexing the diffraction spots, we calculated the apparent size of micelles or more precisely, the center-to-center distance between neighboring micelles. It was 48 nm at pH = 3.11, 45 nm at pH = 4.49, and 44 nm at pH = 5.25. Thus, the results from SAXS studies suggested that the scenario in which both the micelle size and the number of polymer chains decrease with the increase of pH is more likely to be the case. That is, the micelle size decreased slightly but more micelles formed, resulting in a greater volume fraction of micelles in the gel. Since the CGC of a block copolymer in water is determined by the total volume of micelles, it is thus reasonable that the CGC decreases with the increase of pH.

This could also explain the observations in rheological measurements for the samples at three pH values; micelles were more jammed in the gel state at higher pH values, giving rise to higher maximum G' values (Figure 3) and greater viscosities (Figure 5b).

CONCLUSIONS

A well-defined multiresponsive hydrophilic diblock copolymer, P(TEGMA-*co*-AA)-*b*-PDEGEA, was successfully synthesized. A 20 wt % aqueous solution of P(TEGMA-*co*-AA)-*b*-PDEGEA with pH of 3.11 underwent multiple phase transitions upon heating, from a clear, free-flowing liquid (<19 °C), to a clear, free-standing gel (19–39 °C), to a clear, free-flowing hot liquid (40–55 °C), and a cloudy mixture (≥ 56 °C). The data from rheological measurements corroborated the visual examination results. With the increase of pH, the $T_{\text{gel-sol}}$ and the T_{clouding} of the sample shifted to higher temperatures, while the $T_{\text{sol-gel}}$ remained the same. The sol-gel-sol-cloudy transitions and the observed pH effects stemmed from the thermosensitive properties of the two blocks of the diblock copolymer and the pH dependence of the LCST of P(TEGMA-*co*-AA), which were confirmed by DSC and DLS studies. We also determined the sol-gel-sol phase diagrams of P(TEGMA-*co*-AA)-*b*-PDEGEA in water in the moderate concentration range at three pH values (3.11, 4.49, and 5.25). While the lower temperature boundaries overlapped, the upper boundary shifted upward and the CGC decreased with the increase of pH. In contrast, the sol-gel-sol phase diagram of P(TEGMA-*b*-PDEGEA, which contained no pH-responsive groups, showed no changes with pH. SAXS studies suggested that the micelles likely became smaller with the increase of pH and thus more micelles were present in the gel state. This work demonstrated that the sol-gel-sol-cloudy transitions of moderately concentrated aqueous solutions of a thermosensitive hydrophilic diblock copolymer can be tuned by incorporating a small amount of stimuli-responsive groups into a thermosensitive block and applying a second external stimulus. This provides great flexibility for the design of stimuli-responsive reversible gels for potential applications.

ASSOCIATED CONTENT

S Supporting Information. Synthesis of P(TEGMA-*b*-PDEGEA by RAFT, preparation of 20 wt % aqueous solution of P(TEGMA-*b*-PDEGEA, flow curves of 20 wt % aqueous solutions of P(TEGMA-*co*-AA)-*b*-PDEGEA with pH of 4.49 and 5.25, determination of the structure of aqueous micellar gels of P(TEGMA-*co*-AA)-*b*-PDEGEA by small-angle X-ray scattering, and temperature effect on the pH values of a KHP buffer with pH of 3.32 at 0 °C and a 18 wt % aqueous solution of a different but similar P(TEGMA-*co*-AA)-*b*-PDEGEA with pH of 3.05 at 0 °C. This material is available free of charge via the Internet at <http://pubs.acs.org>.

AUTHOR INFORMATION

Corresponding Author

*E-mail: zhao@ion.chem.utk.edu.

ACKNOWLEDGMENT

This work was supported by the National Science Foundation through award DMR-0906913.

REFERENCES

- (1) (a) Hamley, I. W. *Block Copolymers in Solution: Fundamentals and Applications*; John Wiley & Sons: Chichester, U.K., 2005. (b) Hamley, I. W. *Philos. Trans. R. Soc. London A* **2001**, 359, 1017–1044.
- (2) (a) He, C. L.; Kim, S. W.; Lee, D. S. *J. Controlled Release* **2008**, 127, 189–207. (b) Joo, M. K.; Park, M. H.; Choi, B. G.; Jeong, B. *J. Mater. Chem.* **2009**, 19, 5891–5905. (c) Yu, L.; Ding, J. *Chem. Soc. Rev.* **2008**, 37, 1473–1481. (d) Gil, E. S.; Hudson, S. M. *Prog. Polym. Sci.* **2004**, 29, 1173–1222.
- (3) Jeong, B. M.; Bae, Y. H.; Lee, D. S.; Kim, S. W. *Nature* **1997**, 388, 860–862.
- (4) (a) Li, C.; Tang, Y.; Armes, S. P.; Morris, C. J.; Rose, S. F.; Lloyd, A. W.; Lewis, A. L. *Biomacromolecules* **2005**, 6, 994–999. (b) Li, C.; Buurma, N. J.; Haq, I.; Turner, C.; Armes, S. P. *Langmuir* **2005**, 21, 11026–11033. (c) Madsen, J.; Armes, S. P.; Lewis, A. L. *Macromolecules* **2006**, 39, 7455–7457. (d) Kirkland, S. E.; Hensarling, R. M.; McConaught, S. D.; Guo, Y.; Jarrett, W. L.; McCormick, C. L. *Biomacromolecules* **2008**, 9, 481–486. (e) Fechner, N.; Badi, N.; Schade, K.; Pfeifer, S.; Lutz, J.-F. *Macromolecules* **2009**, 42, 33–36.
- (5) (a) Hvidt, S.; Jørgensen, E. B.; Schillén, K.; Brown, W. J. *Phys. Chem.* **1994**, 98, 12320–12328. (b) Mortensen, K.; Brown, W.; Norden, B. *Phys. Rev. Lett.* **1992**, 68, 2340–2343. (c) Mortensen, K. *Europhys. Lett.* **1992**, 19, 599–604. (d) Alexandridis, P.; Hatton, T. A. *Colloids Surf., A* **1995**, 96, 1–46. (e) Wanka, G.; Hoffmann, H.; Ulbricht, W. *Macromolecules* **1994**, 27, 4145–4159. (f) Zhou, Z.; Chu, B. *Macromolecules* **1994**, 27, 2025–2033.
- (6) (a) Li, H.; Yu, G. -E.; Price, C.; Booth, C.; Hecht, E.; Hoffmann, H. *Macromolecules* **1997**, 30, 1347–1354. (b) Alexandridis, P.; Olsson, U.; Kindman, B. *Langmuir* **1997**, 12, 23–34. (c) Hamley, I. W.; Pople, J. A.; Fairclough, J. P. A.; Ryan, A. J.; Booth, C.; Yang, Y.-W. *Macromolecules* **1998**, 31, 3906–3911. (d) Hamley, I. W.; Daniel, C.; Mingvanish, W.; Mai, S.-M.; Booth, C.; Messe, L.; Ryan, A. J. *Langmuir* **2000**, 16, 2508–2514.
- (7) Liu, S.; Billingham, N. C.; Armes, S. P. *Angew. Chem., Int. Ed.* **2001**, 40, 2328–2331.
- (8) (a) Lin, H. H.; Cheng, Y. L. *Macromolecules* **2001**, 34, 3710–3715. (b) Motokawa, R.; Morishita, K.; Koizumi, S.; Nakahira, T.; Annaka, M. *Macromolecules* **2005**, 38, 5748–5760. (c) Sugihara, S.; Hashimoto, K.; Okabe, S.; Shibayama, M.; Kanaoka, S.; Aoshima, S. *Macromolecules* **2004**, 37, 336–343.
- (9) (a) Aoshima, S.; Sugihara, S. *J. Polym. Sci., Part A: Polym. Chem.* **2000**, 38, 3962–3965. (b) Aoshima, S.; Sugihara, S.; Shibayama, M.; Kanaoka, S. *Macromol. Symp.* **2004**, 215, 151–163. (c) Sugihara, S.; Kanaoka, S.; Aoshima, S. *J. Polym. Sci., Part A: Polym. Chem.* **2004**, 42, 2601–2611. (d) Sugihara, S.; Kanaoka, S.; Aoshima, S. *Macromolecules* **2005**, 38, 1919–1927. (e) Aoshima, S.; Kanaoka, S. *Adv. Polym. Sci.* **2008**, 210, 169–208.
- (10) (a) Jiang, X. G.; Lavender, C. A.; Woodcock, J. W.; Zhao, B. *Macromolecules* **2008**, 41, 2632–2643. (b) Jiang, X. G.; Zhao, B. *Macromolecules* **2008**, 41, 9366–9375. (c) Jiang, X. G.; Jin, S.; Zhong, Q. X.; Dadmun, M. D.; Zhao, B. *Macromolecules* **2009**, 42, 8468–8476. (d) O'Lenick, T. G.; Jiang, X. G.; Zhao, B. *Langmuir* **2010**, 26, 8787–8796. (e) Woodcock, J. W.; Wright, R. A. E.; Jiang, X. G.; O'Lenick, T. G.; Zhao, B. *Soft Matter* **2010**, 6, 3325–3336. (f) O'Lenick, T. G.; Jin, N. X.; Woodcock, J. W.; Zhao, B. *J. Phys. Chem. B* **2011**, 115, 2870–2881.
- (11) (a) Zhao, B.; Viernes, N. O. L.; Moore, J. S.; Beebe, D. J. *J. Am. Chem. Soc.* **2002**, 124, 5284–5285. (b) Zhao, B.; Moore, J. S.; Beebe, D. J. *Langmuir* **2003**, 19, 1873–1879. (c) Jiang, J. Q.; Tong, X.; Morris, D.; Zhao, Y. *Macromolecules* **2006**, 39, 4633–4640. (d) Zhao, Y. *J. Mater. Chem.* **2009**, 19, 4887–4895.
- (12) (a) Han, S.; Hagiwara, M.; Ishizone, T. *Macromolecules* **2003**, 36, 8312–8319. (b) Ishizone, T.; Seki, A.; Hagiwara, M.; Han, S.; Yokoyama, H.; Oyane, A.; Deffieux, A.; Carloti, S. *Macromolecules* **2008**, 41, 2963–2967. (c) Lutz, J.-F.; Hoth, A. *Macromolecules* **2006**, 39, 893–896. (d) Lutz, J. F.; Weichenhan, K.; Akdemir, O.; Hoth, A. *Macromolecules* **2007**, 40, 2503–2508. (e) Zhao, B.; Li, D. J.; Hua, F. J.; Green, D. R. *Macromolecules* **2005**, 38, 9509–9517. (f) Hua, F. J.; Jiang, X. G.; Li, D. J.; Zhao, B. *J. Polym. Sci., Part A: Polym. Chem.* **2006**, 44, 2454–2467. (g) Jiang, X. G.; Zhao, B. *J. Polym. Sci., Part A: Polym. Chem.* **2007**, 45, 3707–3721. (h) Allcock, H. R.; Dudley, G. K. *Macromolecules* **1996**, 29, 1313–131. (i) O'Lenick, T. G.; Jiang, X. M.; Zhao, B. *Polymer* **2009**, 50, 4363–4371. (j) Li, D. J.; Zhao, B. *Langmuir* **2007**, 23, 2208–2217. (k) Li, D. J.; Dunlap, J. R.; Zhao, B. *Langmuir* **2008**, 24, 5911–5918. (l) Jiang, X. M.; Wang, B. B.; Li, C. Y.; Zhao, B. *J. Polym. Sci., Part A: Polym. Chem.* **2009**, 47, 2853–2870. (m) Qiao, Z.-Y.; Du, F.-S.; Zhang, R.; Liang, D.-H.; Li, Z.-C. *Macromolecules* **2010**, 43, 6485–6494.
- (13) (a) Chiefari, J.; Chong, Y. K.; Ercole, F.; Krstina, J.; Jeffery, J.; Le, T. P. T.; Mayadunne, R. T. A.; Meijs, G. F.; Moad, C. L.; Moad, G.; Rizzardo, E.; Thang, S. H. *Macromolecules* **1998**, 31, 5559–5562. (b) Moad, G.; Rizzardo, E.; Thang, S. H. *Acc. Chem. Res.* **2008**, 41, 1133–1142.
- (14) (a) Anderson, B. C.; Cox, S. M.; Bloom, P. D.; Sheares, V. V.; Mallapragada, S. K. *Macromolecules* **2003**, 36, 1670–1676. (b) Determan, M. D.; Cox, J. P.; Seifert, S.; Thiagarajan, P.; Mallapragada, S. K. *Polymer* **2005**, 46, 6933–6946. (c) Determan, M. D.; Guo, L.; Thiagarajan, P.; Mallapragada, S. K. *Langmuir* **2006**, 22, 1469–1473.
- (15) (a) Shim, W. S.; Yoo, J. S.; Bae, Y. H.; Lee, D. S. *Biomacromolecules* **2005**, 6, 2930–2934. (b) Shim, W. S.; Kim, S. W.; Lee, D. S. *Biomacromolecules* **2006**, 7, 1935–1941.
- (16) (a) Park, S. Y.; Lee, Y.; Bae, K. H.; Ahn, C. H.; Park, T. G. *Macromol. Rapid Commun.* **2007**, 28, 1172–1176. (b) Suh, J. M.; Bae, S. J.; Jeong, B. *Adv. Mater.* **2005**, 17, 118–120. (c) Joo, M. K.; Park, M. H.; Choi, B. G.; Jeong, B. *J. Mater. Chem.* **2009**, 19, 5891–5905.
- (17) (a) Shim, W. S.; Kim, J. H.; Park, H.; Kim, K.; Kwon, I. C.; Lee, D. S. *Biomaterials* **2006**, 27, 5178–5185. (b) Dayananda, K.; He, C. L.; Park, D. K.; Park, T. G.; Lee, D. S. *Polymer* **2008**, 49, 4968–4973. (c) Huynh, D. P.; Nguyen, M. K.; Kim, B. S.; Lee, D. S. *Polymer* **2009**, 50, 2565–2571.
- (18) Chong, Y. K.; Krstina, J.; Le, T. P. T.; Moad, G.; Postma, A.; Rizzardo, E.; Thang, S. H. *Macromolecules* **2003**, 36, 2256–2272.
- (19) The details and data are included in the Supporting Information.
- (20) All pH values reported in this work were measured at 0 °C. We examined the effect of temperature on pH values of a 20 mM aqueous KHP buffer with pH of 3.32 at 0 °C and a 18 wt% aqueous solution of a different but similar thermo- and pH-sensitive diblock copolymer P(TEGMA-co-AA)-b-PDEGEA with pH of 3.05 at 0 °C. The pH values of these two solutions at 0, 25, 45, and 65 °C were measured. We found that the pH variations were <0.1 for both solutions in the range 0–65 °C. Details can be found in the Supporting Information. In light of this observation, we believe that the temperature-induced pH variations should not affect our conclusions.
- (21) Noro, A.; Matshushita, Y.; Lodge, T. P. *Macromolecules* **2009**, 42, 5802–5810.
- (22) Kossuth, M. B.; Morse, D. C.; Bates, F. S. *J. Rheol.* **1999**, 43, 167–196.
- (23) (a) Yin, X.; Hoffman, A. S.; Stayton, P. S. *Biomacromolecules* **2006**, 7, 1381–1385. (b) Feil, H.; Bae, Y. H.; Feijen, J.; Kim, S. W. *Macromolecules* **1993**, 26, 2496–2500. (c) Bulmus, V.; Ding, Z.; Long, C. J.; Stayton, P. S.; Hoffman, A. S. *Bioconjugate Chem.* **2000**, 11, 78–83. (d) Lokitz, B. S.; York, A. W.; Stempka, J. E.; Treat, N. D.; Li, Y.; Jarrett, W. L.; McCormick, C. L. *Macromolecules* **2007**, 40, 6473–6480. (e) Yamamoto, S.-I.; Pietrasik, J.; Matyjaszewski, K. *Macromolecules* **2008**, 41, 7013–7020. (f) Luo, C. H.; Liu, Y.; Li, Z. B. *Macromolecules* **2010**, 43, 8101–8108.
- (24) Bai, Z. F.; Lodge, T. P. *J. Phys. Chem. B* **2009**, 113, 14151–14157.
- (25) The crossover of G' and G'' curves was not observed on the high temperature side. We repeated the measurement several times and the results were reproducible. The reason is unclear at present.
- (26) Schild, H. G. *Prog. Polym. Sci.* **1992**, 17, 163–249.
- (27) Urry, D. W. *J. Phys. Chem. B* **1997**, 101, 11007–11028.
- (28) The third possible scenario is that both the number of polymer molecules in each micelle and the size of micelles increase with the increase of pH. This scenario is unlikely the case. The ionization of carboxylic acid groups at a higher pH would lead to the P(TEGMA-co-AA) block occupying a larger volume while the PDEGEA block stays the same, which should favor micelles with a larger curvature (a smaller size).